Numerical simulation of the trapping reaction with mobile and reacting traps

Joshua D. Hellerick,[1] Robert C. Rhoades,[2] and Benjamin P. Vollmayr-Lee [1,*]

[1]*Department of Physics, Bucknell University, Lewisburg, Pennsylvania 17837, USA*
[2]*Susquehanna International Group, Bala Cynwyd, Pennsylvania 19004, USA*

We study a variation of the trapping reaction, $A + B \rightarrow A$, in which both the traps (A) and the particles (B) undergo diffusion, and the traps upon meeting react according to $A + A \rightarrow 0$ or A. This two-species reaction-diffusion system is known to exhibit a nontrivial decay exponent for the B particles, and recently renormalization group methods have predicted an anomalous dimension in the BB correlation function. To test these predictions, we develop a computer simulation method, motivated by the technique of Mehra and Grassberger [Phys. Rev. E **65**, 050101(R) (2002)], that determines the complete probability distribution of the B particles for a given realization of the A-particle dynamics, thus providing a significant increase in the quality of statistics. Our numerical results indeed reveal the anomalous dimension predicted by the renormalization group, and compare well quantitatively to precisely known values in cases where the problem can be related to a four-walker problem.
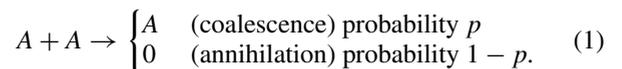
I. INTRODUCTION

Reaction-diffusion processes with irreversible reactions provide an important class of far-from-equilibrium systems. Interest in these systems stems from the fact that the particles develop nontrivial correlations that cannot be described by equilibrium fluctuations, and these correlations in turn affect the reaction rates and particle densities. Applications for these model systems include chemical reaction kinetics [1], interface growth models [2], aggregation [3], domain coarsening [4], and population dynamics [5].

In the present paper, we consider a two-species process consisting of the trapping reaction $A + B \rightarrow A$, in which A particles, or "traps," catalyze the decay of B particles, and where the traps additionally react according to $A + A \rightarrow 0$ (annihilation) or $A + A \rightarrow A$ (coalescence). Both particle types A and B undergo diffusion with corresponding diffusion constants D_A and D_B. This system has been predicted via renormalization group (RG) methods to exhibit anomalous dimensions in both the B-particle density decay [6–8] and separately in the scaling of the BB correlation function [9] for spatial dimension $d < 2$. The primary focus of this paper is to test these predictions numerically in one- and two-dimensional systems. For this purpose, we develop a hybrid Monte Carlo technique that provides the entire B-particle distribution for a given realization of the A particles. This is possible because, as argued below, the B particles remain locally Poissonian. As a result, we have obtained precise numerical measurements of the particle statistics for this reaction with mobile B particles in $d = 1$ and $d = 2$.

For the $A + B \rightarrow A$ trapping reaction with mobile but *nonreacting* traps, the mean-field rate equation predicts the

B-particle density to decay exponentially with time. However, scaling arguments and rigorous bounds confirm that for dimension $d \leqslant 2$ nontrivial correlations develop between the traps and the surviving B particles, invalidating the rate equation and causing the B-particle density to decay as a stretched exponential $\langle b \rangle \sim \exp(-\lambda_d t^{d/2})$ for $d < 2$ [with logarithmic corrections $\langle b \rangle \sim \exp(-\lambda_2 t / \ln t)$ in $d = 2$] and with a universal coefficient λ_d [10–13]. Here and throughout, angle brackets are used to indicate averages over the random initial conditions and over the stochastic processes of reaction and diffusion.

Now consider traps that are additionally reacting according to

$$A + A \rightarrow \begin{cases} A & \text{(coalescence) probability } p \\ 0 & \text{(annihilation) probability } 1 - p. \end{cases} \quad (1)$$

Since the traps are unaffected by the B particles, their dynamics reduces to the well-studied single-species reaction, where mean-field rate equations (see below), exact solutions in one spatial dimension [14–16], and field-theoretic RG methods [17–19] for general dimension demonstrate that the A particle density decays as power law (with a multiplicative logarithmic correction in $d = 2$). This decaying trap density then enhances the survival probability of the B particles, resulting in a power law decay with time, $\langle b \rangle \sim t^{-\theta}$. For example, the rate equations, valid for $d > 2$ where diffusion manages to keep the reactants well mixed, are

$$\partial_t \langle a \rangle = -\Gamma \langle a \rangle^2, \qquad \partial_t \langle b \rangle = -\Gamma' \langle a \rangle \langle b \rangle, \quad (2)$$

with solutions $\langle a \rangle \sim 1/(\Gamma t)$ and $\langle b \rangle$ decay exponent determined by the nonuniversal rate constants, $\theta = \Gamma'/\Gamma$.

For $d < 2$, the depletion caused by reactions competes with diffusion, developing correlations that modify the reaction rate. This results in the trap density decay $\langle a \rangle \sim A_d (D_A t)^{-d/2}$ with a universal coefficient A_d. The B particle density in this fluctuation-dominated case has been studied with

*ben.vollmayr-lee@bucknell.edu

Smoluchowski theory [20], which is an improved rate equation that incorporates the depletion with a time-dependent rate constant, and with RG techniques [6–9]. In both cases, the B particle density was found to decay as a power law with a universal exponent θ depending only on the diffusion constant ratio $\delta = D_B/D_A$ and the trap reaction parameter p defined in Eq. (1). Smoluchowski theory gives

$$\theta_S = \frac{d}{2-p}\left(\frac{1+\delta}{2}\right)^{d/2} \qquad (3)$$

while the RG analysis predicts

$$\theta = \theta_S + \tfrac{1}{2}\gamma_b^*, \qquad (4)$$

where γ_b^* is an anomalous dimension of order $\epsilon = 2 - d$ which stems from a field renormalization of the density [7,9].

In the case of $d = 2$, the B particle density is predicted by RG methods [8] to decay as

$$\langle b(t) \rangle \sim t^{-\theta}|\ln t|^{\alpha}, \qquad (5)$$

with $\theta = (1 + \delta)/(2 - p)$. The logarithm power α is found to be nonuniversal and related to the microscopic reaction rate constants.

This model reduces in the limit of $\delta \to 0$ ($D_B \to 0$) to a study of persistence (see Ref. [13] for a recent review). That is, the B particles simply become stationary markers, and their survival to time t indicates that no A particle has visited that particular site. Thus the exponent θ becomes the persistence exponent for the single-species reaction $A + A \to 0, A$.

Recently, it was shown by RG methods that an additional anomalous dimension occurs due to the field renormalization of the b^2 density operator [9], with the consequence that the B-particle correlation function scales for $d < 2$ as

$$C_{BB}(r,t) \equiv \frac{\langle b(r,t)b(0,t)\rangle - \langle b(t)\rangle^2}{\langle b(t)\rangle^2} \sim t^{\phi}f(r/\sqrt{t}), \qquad (6)$$

where ϕ is a universal exponent of order ϵ. In contrast, the scaled correlation functions C_{AA} and C_{AB} are simply functions of $r/\sqrt{t}$ with no time-dependent prefactor. We note that $\chi_{BB}(t) \equiv C_{BB}(0,t)$ is a measure of the local fluctuations, and Eq. (6) predicts that χ_{BB} grows as a universal power of time. In dimension $d = 2$, the correlation function scales as

$$C_{BB}(r,t) \sim |\ln t|^{\beta}f(r/\sqrt{t}). \qquad (7)$$

In Ref. [9], the exponent ϕ was computed to first order in ϵ and an explicit expression for β was obtained. Additionally, an exact value of ϕ was obtained for the case of $p = \delta = 1$ in one spatial dimension by mapping to a four-walker problem [9] and solving an eigenvalue problem numerically [21].

Here we aim to use numerical simulations to test the predicted scaling forms Eqs. (6) and (7) and to measure the exponents θ, ϕ, α, and β. These simulations are challenging since the window of scaling behavior is limited by transients at early times and finite-size effects and vanishing particle numbers at late times. In the present paper, we circumvent the small number statistics of the B particles by determining the entire B-particle probability distribution conditioned on a particular realization of the A-particle dynamics. Our technique was inspired by and is a converse to the method of Mehra and Grassberger [22], who studied the trapping reaction by

monitoring a single particle and updating the distribution of traps. With greatly improved statistical accuracy, we were able to demonstrate the scaling collapse of the AA, AB, and BB correlation functions and measure the dynamical exponents θ and ϕ to high accuracy.

The layout of this paper is as follows. In Sec. II, we present our hybrid simulation method, which also serves to define the model we are considering. In Sec. III, we report our measurements of the density decay exponent θ for $d = 1$ for a variety of δ and p values, and compare these to known exact solutions, RG calculations, and the Smoluchowski approximation. Then in Sec. IV we present our data for the anomalous dimension ϕ in $d = 1$, and compare to the RG prediction and the exact solution from the four-walker problem, while in Sec. V we test the pair correlation functions for scaling collapse. In Sec. VI, we present simulations in $d = 2$ and compare the exponents and logarithmic corrections to the explicit RG predictions. Finally, in Sec. VII we summarize our results and suggest future work.

II. HYBRID MONTE CARLO AND MASTER EQUATION METHOD

Reaction-diffusion systems are typically simulated via Monte Carlo methods: A lattice is populated randomly by particles and then updated according to the particular rules for reaction and stochastic diffusion. Quantities of interest are then averaged over multiple realizations of the stochastic processes. Monte Carlo is employed rather than direct computation of the probabilities in a master equation because of the impossibility of dealing with such a large number of configurations.

However, for the trapping reaction, the B particles are noninteracting and this allows for a much simpler description of the B-particle probabilities. We use this to construct a hybrid approach in which we use Monte Carlo for the A particles, but for each realization of the A-particle dynamics we calculate the entire B-particle probability distribution. This is possible because the B-particle distribution remains Poissonian at each lattice site.

We now define our model for concreteness. We consider a d-dimensional hypercubic lattice and use a parallel update, as illustrated in Fig. 1. In $d = 1$, the particles are initially located on even-numbered lattice sites. In higher dimensions, the particles are initially located on sites whose lattice indices sum to an even number, e.g., the black squares of a checkerboard for $d = 2$. For the A particles, we start with every allowed site singly occupied. For the B particles, we will be tracking a distribution, and our initial condition is a Poissonian distribution of the unit mean at each allowed site.

In a diffusion step, each particle will simultaneously hop in one of the $\pm \hat{x}_i$ directions along the principle axes of the lattice, so after an even (odd) number of steps, the particles reside in the even (odd) sector of the bipartite lattice. Reactions are then performed subsequent to the diffusion hops. In the simplest scenario, for any site containing both A and B particles, the B particles are removed. A variant of this rule would be for each B particle to be removed with probability p'. Any site containing two A particles reacts according to Eq. (1), governed by the parameter p.
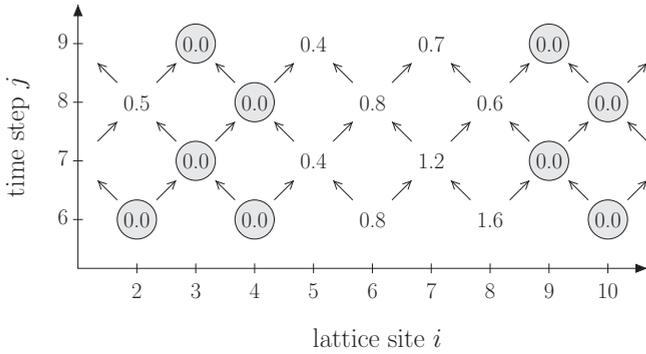
FIG. 1. An illustration of the parallel update in $d = 1$. All particles occupy even (odd) numbered sites at even (odd) numbered time steps. The circles represent A particles, with an $A + A \rightarrow A$ reaction occurring at site $i = 3$ and time step $j = 7$. The numbers represent the means of the Poisson distribution of B particles, which are updated according the rules in Eqs. (8) and (9), with $p' = 1$.

When the A and B diffusion constants are equal, both particle types step simultaneously, resulting in the diffusion constant $D = \Delta x^2 / (2d \Delta t)$ for a lattice constant Δx and a hop time Δt. For unequal diffusion constants, we can take an odd number of multiple steps for one of the species. For example, if $\delta = D_B / D_A = 3$ we take two steps with the B particles, check the $A + B \rightarrow B$ reaction, take one more step with both particle types, and then check the reactions again. For $\delta = 2$, we first do the process just described and then take one more step with both particle types. In this way, any rational value of the diffusion constant ratio δ can be realized.

Our hybrid technique relies on the following two well-known properties of Poisson distributions:

P1. The sum of two independent Poisson distributed random variables with mean values μ and ν is a Poisson random variate with mean $\mu + \nu$.

P2. The compound of a Poisson distribution with mean μ and a binomial distribution with probability q is a Poisson distribution with mean $q\mu$.
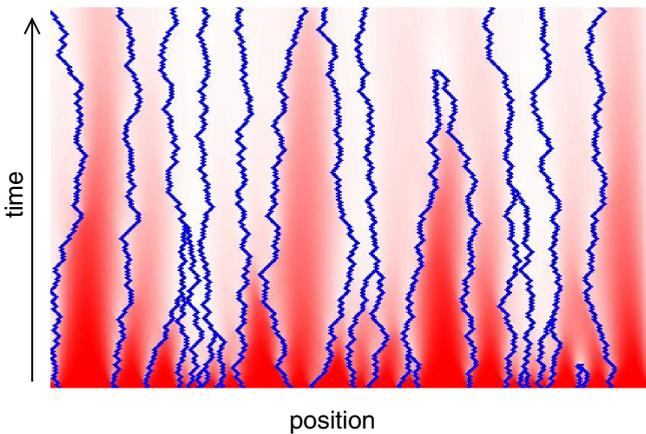

FIG. 2. A characteristic segment of our simulation. The blue lines are A particles (traps), which undergo both coalescence and annihilation reactions. The B-particle probability distribution is shaded in red, with the intensity representing the local Poissonian mean.

The second property says that if a number of elements is a Poissonian random variate and then a random subset of elements are selected with independent probabilities, the selected number of elements is a Poissonian random variate.

Now assume at some time t the B particles are Poisson distributed on each lattice site i with a mean value b_i. In the subsequent diffusion step, the probability of a particle making the hop from site i to a particular nearest-neighbor j is $1/(2d)$. Thus, from property P2, these particles will contribute a Poisson distributed number of particles with mean $b_i/(2d)$ to each of their neighboring sites. The new distribution at a particular site j is a sum of Poisson random variates, thus, by property P1, it is Poissonian with mean given by

$$b_{j,t+\Delta t} = \frac{1}{2d} \sum_k b_{k,t}, \tag{8}$$

where k are the nearest neighbors of j.

To incorporate the trapping reaction, we take

$$b_{i,t} \rightarrow (1 - p') b_{i,t} \tag{9}$$

at any site i containing an A particle at time t, which derives from property P2, recalling that each B particle independently reacts with probability p', or survives with probability $1 - p'$.

Thus, we find that dynamical process preserves the locally Poissonian character of the B particle distribution. Since we start from Poissonian initial conditions, then by induction the Poissonian measure is preserved for all times.

With this method, an explicit realization of the A particles is evolved, and simultaneously the local means of the Poissonian B particles are updated by use of Eqs. (8) and (9). A visualization of a simulation in $d = 1$ is presented in Fig. 2. The computational cost of this method in comparison to a Monte Carlo simulation of the B particles is the introduction of a floating point variable that has to be updated at each lattice site at each time step. The gain is vastly improved statistics, particularly for parameter values where θ is large, for which the B-particle density decays rapidly and Monte Carlo simulations would yield vanishing particle numbers.

III. B-PARTICLE DENSITY IN $d = 1$

We measured the B-particle density for one-dimensional systems with lattice size ranging from 10^6 up to 3×10^7 sites. We set $\Delta x = \Delta t = 1$ and used an initial condition of $\langle a(0) \rangle = 0.5$ for the trap density and without loss of generality we set $\langle b(0) \rangle$ to unity.

Simulations were performed for diffusion constant ratios $\delta = D_B / D_A = 1/4, 1/2, 1, 2,$ and 4 for both the $A + A \rightarrow 0$ ($p = 0$) and the $A + A \rightarrow A$ ($p = 1$) trap reactions. Additionally, for equal diffusion constants $\delta = 1$, we simulated mixed trap reactions with $p = 1/4, 1/2,$ and $3/4$, with p defined in Eq. (1). We also varied the trapping probability parameter p' in Eq. (9) to confirm the universality of our results. The data presented here and below correspond to $p' = 1$. In each case, we performed between 100 and 400 independent runs. For the statistical uncertainties at different times to be uncorrelated, we used an independent set of runs for each time value where we collected data. The onset time for finite-size effects depended strongly on the parameters δ and p, decreasing with respect to both parameters. As such, we chose the system size
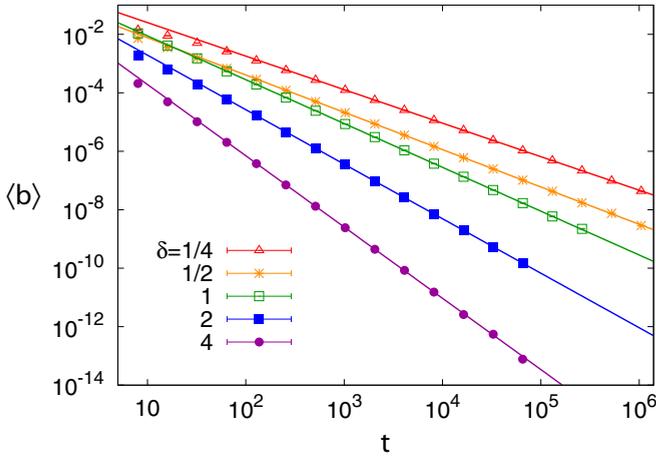
FIG. 3. Log-log plot of the average B-particle density versus time in $d = 1$, demonstrating multiple decades of scaling for the case $p = 1$ (traps undergoing $A + A \rightarrow A$) for various diffusion constant ratios $\delta = D_B/D_A$. The error bars are significantly smaller than the points plotted.

and simulation run time accordingly for each parameter set to optimize the scaling regime.

Representative data for the B-particle density with $p = 1$ and varying δ values are presented in Fig. 3, along with the best-fit power law. Not all data points shown are used in the fits.

We fit our data with independent errors at each time value to a power law, choosing our minimum and maximum times according to goodness of fit. We estimated the uncertainty of the exponent by varying the minimum and maximum times. We can evaluate the effectiveness of this procedure by comparing to two exact solutions:

(1) For $p = 1$, the B-particle density decays like the survival probability in a three-walker problem [23], giving

$$\theta = \frac{\pi}{2 \arccos[\delta/(1 + \delta)]}. \tag{10}$$

(2) For $p = 0$ and $\delta = 1$, the B particles behave exactly like A particles: An A particle surviving until time t has executed a random walk among the other A particles undergoing the $A + A \rightarrow 0$ reaction without meeting another particle. The same statement applies to B particles, so they have the same survival probability. This implies $\langle b \rangle \sim \langle a \rangle$, giving $\theta = 1/2$.

Our measured values along with their uncertainties are reported in Table I. The uncertainty estimates appear to be reasonable.

Theoretical results for θ include the exact solutions described above, as well as Smoluchowski theory, which provides the value θ_S given in Eq. (3), and the RG $\epsilon = 2 - d$ expansion. Smoluchowski theory has proved to be surprisingly effective, e.g., it correctly predicts the A-particle decay exponent for all dimensions [20], but is an uncontrolled approximation. By contrast, the RG ϵ expansion is systematic, but has only been computed to first order in ϵ [6,8,9]. For completeness, we provide the result here:

$$\theta = \theta_S + \frac{1}{4}\left[\frac{1+\delta}{2-p} + \left(\frac{1+\delta}{2-p}\right)^2 f(\delta)\right]\epsilon + O(\epsilon^2), \tag{11}$$

TABLE I. Measured values of θ in $d = 1$ for various diffusion constant ratios $\delta = D_B/D_A$ and trap reaction parameter p, defined in Eq. (1). The exact values from the vicious walker problem are included for comparison.

δ	p	θ_{measured}	θ_{exact}
1/4	0	0.4129(7)	
1/2	0	0.4434(4)	
1	0	0.5004(3)	0.5
2	0	0.5899(7)	
4	0	0.7285(9)	
1/4	1	1.1468(7)	1.14704
1/2	1	1.2768(9)	1.27607
1	1	1.4992(9)	1.5
2	1	1.8650(11)	1.86762
4	1	2.438(2)	2.44102
1	1/4	0.5923(3)	
1	1/2	0.7299(10)	
1	3/4	0.9581(16)	

where

$$f(\delta) = 1 + 2\delta\left[\ln\left(\frac{2}{1+\delta}\right) - 1\right]$$
$$+ (1 - \delta^2)\left[\text{Li}_2\left(\frac{\delta - 1}{\delta + 1}\right) - \frac{\pi^2}{6}\right] \tag{12}$$

and $\text{Li}_2(v) = -\int_0^v du \, \ln(1 - u)/u$ is the dilogarithm function [24].

For coalescing traps, $A + A \rightarrow A$, Smoluchowski theory in $d = 1$ and the truncated RG expansion with $\epsilon = 1$ can be compared directly to the vicious walker result, as was done in Ref. [8]. We reproduce the comparison here as the upper curves in Fig. 4 and add to the plot our measured values.
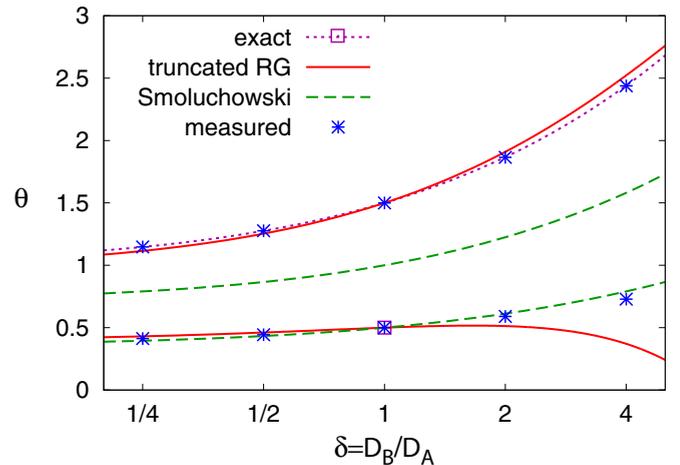

FIG. 4. Measured values of the B-particle decay exponent θ in $d = 1$ plotted versus the diffusion constant ratio, along with the Smoluchowski prediction, Eq. (3), the RG expansion truncated at first order in $\epsilon = 2 - d$, and exact solutions. The upper (lower) curves and points correspond to the $A + A \rightarrow A$ ($A + A \rightarrow 0$) trap reaction. The error bars on the data are much smaller than the points plotted.
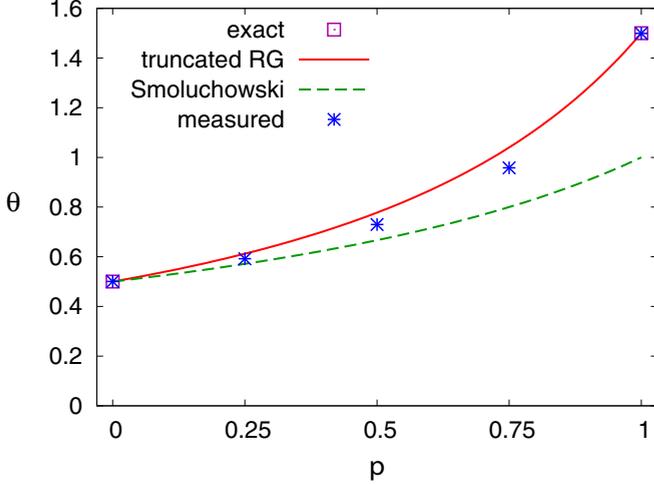
FIG. 5. A similar comparison as in Fig. 4 for the equal diffusion constant case $\delta = 1$ and varying p as defined in Eq. (1).

Primarily, this demonstrates that our simulations and data analysis technique are accurate. Also, as noted in Ref. [8], the truncated RG does a remarkable job of matching the exact solution, while the Smoluchoswki result is considerably low.

The lower set of curves and points in Fig. 4 are the corresponding θ values for annihilating traps, $A + A \rightarrow 0$, where the vicious walker solution is not available. Our measured values for θ indicate that the Smoluchowski approximation, while faring poorly for $p = 1$, is reasonably accurate for $p = 0$. The nonmonotonicity of θ with respect to δ in the truncated RG is likely an artifact of the truncation at $O(\epsilon)$.

Finally, in Fig. 5 we present a similar comparison for the case of equal diffusion constants but varying p. Curiously, the truncated RG expansion matches the exact solutions available at $p = 0$ and $p = 1$, while faring reasonably in between.

IV. ANOMALOUS DIMENSION ϕ IN $d = 1$

From the field theoretic RG calculation, it was determined that b^2, the square of the field associated with the B density, must be renormalized independently of the b itself. A consequence of this renormalization is that the local fluctuations grow as a power law in time, as measured by

$$\chi_{BB}(t) = \frac{\langle b^2 \rangle - \langle b \rangle^2}{\langle b \rangle^2} \sim t^{\phi}, \tag{13}$$

in contrast to the analogous measures

$$\chi_{AA} = \frac{\langle a^2 \rangle - \langle a \rangle^2}{\langle a \rangle^2} = -1 \tag{14}$$

and

$$\chi_{AB} = \frac{\langle ab \rangle - \langle a \rangle \langle b \rangle}{\langle a \rangle \langle b \rangle} = -1, \tag{15}$$

which maintain constant values [9]. Our measured values for χ_{BB} versus time are plotted in Fig. 6, for the case of coalescing traps ($p = 1$). We observe power-law behavior until the onset of finite-size effects. Curiously, finite-size effects appear much earlier in χ_{BB} than they do in the density, by a factor of 10^2 or 10^3 (compare Fig. 3).
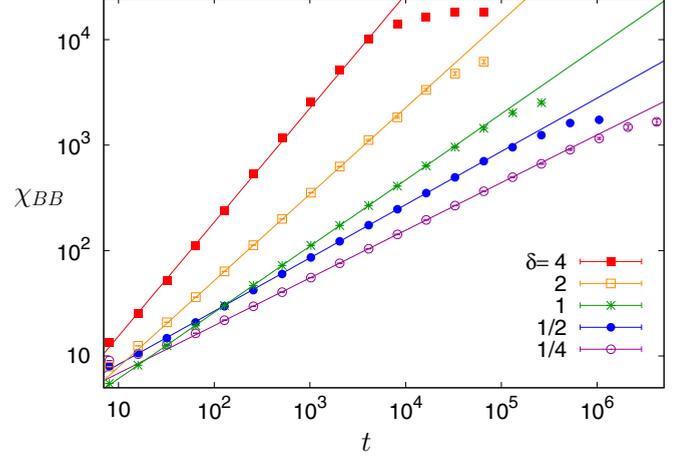

FIG. 6. Log-log plot of the local fluctuations χ_{BB} in $d = 1$ plotted versus time, for the case $p = 1$ and varying δ. The straight lines are power law fits. Finite-size effects are visible at later times, and these data are not included in the fits.

We were unable to demonstrate power-law behavior in χ_{BB} when the traps are annihilating ($p = 0$) or for any of the mixed reactions we simulated ($p = 0.25$, 0.5, and 0.75); our data are consistent with an asymptotic approach to a power law with a small exponent ϕ.

Our measured values of ϕ for $p = 1$ are reported in Table II. Our uncertainties were estimated by varying the fitting range within the scaling regime. For the case $\delta = 1$, an exact value of ϕ can be obtained by considering a four-walker problem, where the walkers on a line are in the order A-B-B-A. The bracketing A walkers are unaffected by any subsequent coalescence events with exterior A particles, so they may be regarded as simple random walkers. The B-particle density squared will decay as the probability for the two interior walkers to survive until and meet at time t [9]. This exponent can be reduced to an eigenvalue problem [21] and the corresponding value is reported in Table II.

The RG calculation of ϕ in Refs. [9] gives

$$\phi = \frac{7}{24 - 18p} \epsilon + O(\epsilon^2), \tag{16}$$

where $\epsilon = 2 - d$. The truncated expansion does not compare well quantitatively with our data, most notably in the absence of δ dependence. Plugging in $\epsilon = 1$ gives $\phi = 7/6 \simeq 1.17$, which is significantly higher than the values we measured. A

TABLE II. Measured values of ϕ in $d = 1$ for various diffusion constant ratios $\delta = D_B/D_A$ and trap reaction parameter $p = 1$, defined in Eq. (1). The exact value from the four-walker problem is included (to seven digits) for comparison.

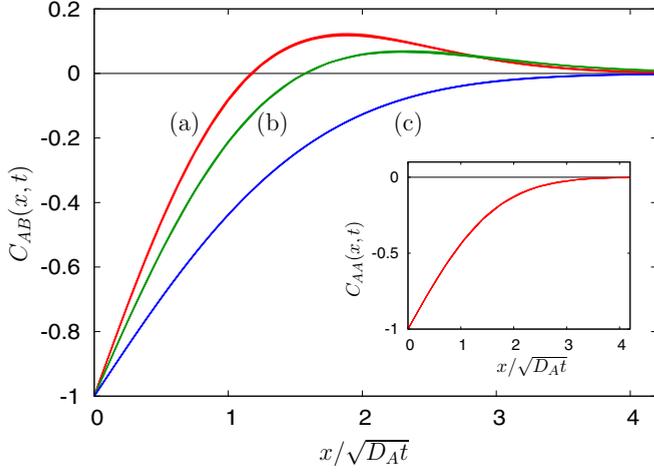| δ	$\phi_{measured}$	ϕ_{exact}
1/4	0.452(2)	
1/2	0.505(3)	
1	0.628(3)	0.6262475
2	0.820(5)	
4	1.08(4)	

FIG. 7. Scaling collapse of the measured correlation functions in $d = 1$ for times ranging over three decades. The cross correlation function $C_{AB}(x, t)$ parameters are (a) $p = 1$, $\delta = 1/4$, (b) $p = 1$, $\delta = 1$, and (c) $p = 0$, $\delta = 1$. The inset shows the measured $C_{AA}(x, t)$ for $p = 0$, $1/2$, and 1, as well as the exact solution, Eq. (18), with striking agreement.
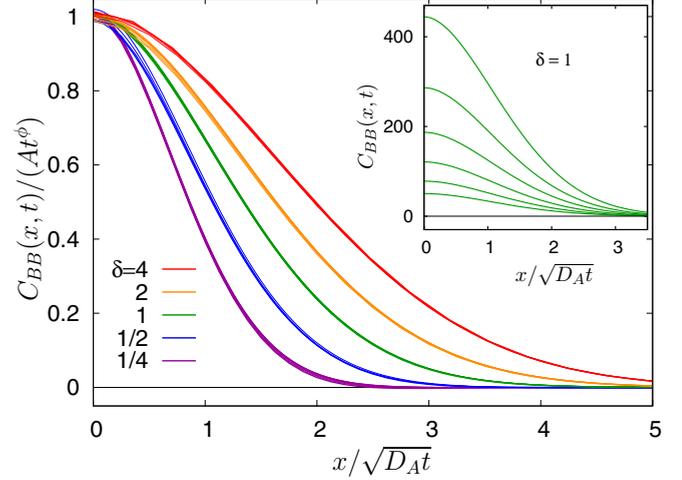

FIG. 8. Scaling collapse of the measured correlation functions $C_{BB}(x, t)$ in $d = 1$ for times ranging over two decades, which requires rescaling the vertical axis by $\chi_{BB} \sim At^\phi$. All plots are for coalescing traps ($p = 1$). The inset shows C_{BB} for $\delta = 1$ without the vertical rescaling; the intercept is increasing with time.

qualitative feature that the RG calculation does capture is that ϕ is a strongly decreasing function of p. Presumably, the RG ϵ expansion is poorly convergent, as was found with the simple annihilation reaction [18].

V. CORRELATION FUNCTIONS IN $d = 1$

Associated with power-law behavior with universal exponents is the phenomenon of dynamical scaling. These share a common origin in the underlying RG fixed point that controls the asymptotic dynamics and structure. We test for this dynamical scaling by measuring the trap and particle two-particle correlation functions, as well as their cross-correlation function.

We first consider the traps, which undergo the single-species $A + A \rightarrow 0, A$ reactions. An exact solution for the correlation function in $d = 1$ was obtained by Masser and ben-Avraham, with the result [25]

$$C_{AA}(x, t) = \frac{\langle a(x, t)a(0, t)\rangle - \langle a(t)\rangle^2}{\langle a(t)\rangle^2} \sim f_{AA}(x/\sqrt{D_A t}),$$
(17)

where

$$f_{AA}(z) = -e^{-z^2/4} + \sqrt{\frac{\pi}{8}} z e^{-z^2/8} \operatorname{erfc}(z/\sqrt{8}).$$
(18)

Interestingly, this result applies to both annihilating and coalescing particles, as well as mixed reactions. We measured these correlation functions via the Monte Carlo realization of our trap dynamics and found convincing scaling collapse and perfect agreement with the exact solution, as shown in the inset of Fig. 7.

We next turn to the cross-correlation function

$$C_{AB}(x, t) = \frac{\langle a(x, t)b(0, t)\rangle - \langle a(t)\rangle\langle b(t)\rangle}{\langle a(t)\rangle\langle b(t)\rangle},$$
(19)

which is plotted in Fig. 7. With our hybrid simulation method, we measure the correlation between the realized A particles and the associated B probability distribution. The data again exhibit convincing scaling collapse, with a scaling function that depends on the parameters δ and p. Both C_{AA} and C_{AB} exhibit anticorrelations at short distances, a direct consequence of the $A + A \rightarrow (0, A)$ and $A + B \rightarrow A$ reactions. However, depending on the parameter values, the cross-correlation function C_{AB} can be nonmonotonic with positive correlations at larger separation. We depict three choices of parameters in Fig. 7, but we found similar scaling collapse for all investigated cases.

Finally, we turn to the B-particle correlation function defined in Eq. (6) and measured by the sampled set of B-particle distributions. Since the B particles do not react with each other, we do not expect them to be anticorrelated at short distances. Instead, a surviving B particle is likely to be found in a region with few A traps nearby, which results in an enhanced probability of other B particles nearby, i.e., positive correlations.

Our measured values for correlation function confirm this, as shown in Fig. 8. The inset shows that when $C_{BB}(x, t)$ is plotted versus the scaled distance $x/\sqrt{D_A t}$, as was done in Fig. 7, we do not find collapse, but rather the correlations are growing in magnitude with time. However, when we also scale the vertical axis by the expected $\chi_{BB} \sim At^\phi$, with A and ϕ taken from our fitted values, we indeed see scaling collapse, as shown in the main part of Fig. 8. Thus, we have confirmed the RG prediction of the scaling form in Eq. (6).

The scaled correlations for $p = 1$ show a significant dependence on the diffusion constant ratio. The similarity of the scaling functions suggest that a rescaling of the horizontal axis to the form $x/\sqrt{D_A^{1-k} D_B^k t}$ might collapse all measured functions to a single curve. Indeed, the value $k = 0.60$ comes close though slight differences are observable. Evidently, the power-law dependence captures a dominant feature of the

δ dependence on the scaling function, but is not an exact result and there is currently no theoretical basis to expect such behavior.

When $p < 1$, we cannot make a scaling plot similar to Fig. 8 since we are unable to simulate late enough to get into the regime where χ_{BB} is a power law. If we instead rescale the vertical scale by $C_{BB}(0, t)$ we find reasonable scaling collapse, suggesting the shape of the correlation function converges more quickly than χ_{BB} itself.

VI. AT THE UPPER CRITICAL DIMENSION $d = 2$

Generally, critical exponents are continuous functions of dimension, changing from their fluctuation-dominated value below the upper critical dimension d_c to their mean-field value for $d > d_c$, while at $d = d_c$ multiplicative logarithmic corrections appear. The A particle density conforms to this, with power-law decay $t^{-d/2}$ for $d < 2$, rate equation behavior t^{-1} for $d > 2$, and the calculated density for $d = 2$ of

$$\langle a(t) \rangle = \frac{1}{4\pi(2-p)} \frac{\ln(t/\tau)}{D_A t}, \quad (20)$$

with a universal prefactor [14,18,26]. The time constant τ is nonuniversal, and provides a subasymptotic correction to scaling.

In contrast, the B-particle density decay exponent θ is universal for $d < 2$, given by Eq. (11), but for $d > 2$ is given by $\theta = \Gamma'/\Gamma$, where Γ and Γ' are nonuniversal constants in the rate equations Eqs. (2). Thus, θ is necessarily discontinuous at d_c. As a consequence, Rajesh and Zaboronski [8] found the density in $d = 2$ to decay as

$$\langle b(t) \rangle \sim t^{-\theta_2} |\ln t|^\alpha, \quad (21)$$

with universal exponent

$$\theta_2 = \lim_{d \to 2^-} \theta = \frac{1+\delta}{2-p}, \quad (22)$$

and with α related to the nonuniversal local rate constants λ and λ':

$$\alpha = \left(\frac{1+\delta}{2-p}\right)\left[\frac{3}{2} + \ln\left(\frac{1+\delta}{2}\right) + \frac{1}{2}\left(\frac{1+\delta}{2-p}\right)f(\delta)\right] \\ - \frac{4\pi(1+\delta)}{2-p}\left(\frac{1}{\lambda} - \frac{1+\delta}{\lambda'}\right), \quad (23)$$

where $f(\delta)$ is given by Eq. (12).

Finally, the anomalous dimension ϕ characterizing the B-particle fluctuations $\chi_{BB} \sim t^\phi$ is continuous at $d = 2$: the RG result for $d < 2$ Eq. (16) is of order $\epsilon = 2 - d$ and so vanishes as $d \to 2^-$, while the rate equations, which contain no fluctuations, give $\phi = 0$ for $d > 2$. At $d = 2$, the RG calculation [9] predicts $\chi_{BB} \sim |\ln t|^\beta$, with

$$\beta = -\frac{5 - 9p}{12 - 9p}. \quad (24)$$

As a consequence, the $C_{BB}(r, t)$ correlation function is expected to scale in $d = 2$ as per Eq. (7), while $C_{AA}(r, t)$ and $C_{AB}(r, t)$ scale as

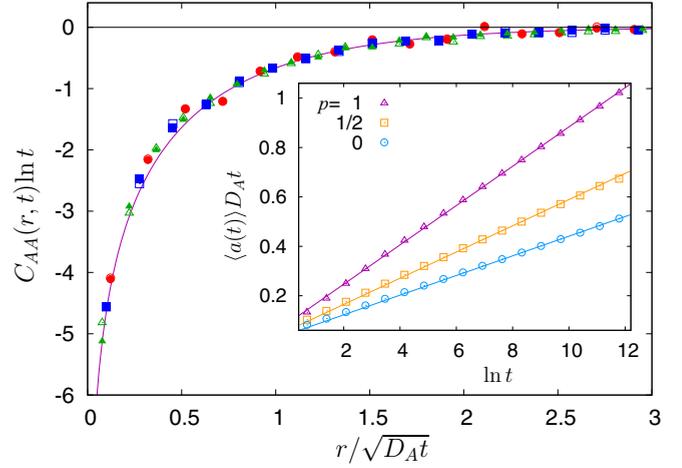$$C_{AA}(r, t) = |\ln t|^{-1} f_{AA}(r/\sqrt{D_A t}), \quad (25)$$

FIG. 9. Scaling plot of $C_{AA}(r, t) \times \ln t$ versus $r/\sqrt{D_A t}$ in $d = 2$ for times $t = 8192$ (○), 32 768 (□), and 131 072 (△), for both $p = 0$ (open symbols) and $p = 1$ (solid symbols). The solid line is the RG result Eq. (27) from Ref. [18]. The inset shows the density $\langle a(t) \rangle D_A t$ plotted versus $\ln t$ for $p = 0$, 1/2, and 1, with the solid lines a one-parameter fit of the RG result Eq. (20).

$$C_{AB}(r, t) = |\ln t|^{-1} f_{AB}(r/\sqrt{D_A t}). \quad (26)$$

In Ref. [18], the Fourier transform of f_{AA} was calculated via RG methods, which we inverse transform here to obtain

$$f_{AA}(z) = e^{-z^2/8}\left(\frac{3}{2} + \frac{z^2}{16}\right) - \Gamma(0, z^2/8)\left(1 + \frac{z^2}{4} + \frac{z^4}{128}\right), \quad (27)$$

where $\Gamma(a, x)$ is the incomplete gamma function [24]. As with $d = 1$, the correlation function does not depend on the value of p.

We now compare these predictions to our numerical results. We used a square lattice of size 4096×4096 evolved to time $t = 131\,072$, with 100 independent runs for each parameter set and for each time point where we collect data (so the errors are uncorrelated). To reduce noise in the purely Monte Carlo measurement of the A particle correlations, we conducted 1000 runs each of the $A + A \to 0$ and $A + A \to A$ reactions.

We first present the A-particle simulations. As shown in Fig. 9, the A-particle correlation function exhibits the expected scaling collapse, and agrees reasonably well with the theoretical prediction Eq. (27). The inset of Fig. 9 shows the A-particle density scaled by a factor of $D_A t$ plotted versus $\ln t$. The solid straight lines represent the theoretical result Eq. (20) with the value of τ fitted to the data. Note that τ only affects the intercept of the lines; the slope is determined by the universal prefactor in Eq. (20). The agreement is quite good. This represents, to our knowledge, the first numerical test of this p-dependent prefactor.

Turning to the B-particle density, we first conducted simulations with infinite local reaction rates $\lambda, \lambda' \to \infty$, which corresponds to reactions occurring with probability unity whenever the particles meet. In this limit, the last, nonuniversal term in Eq. (23) for α vanishes. We fit our data for $t \geqslant t_{\min}$ to the asymptotic form $\langle b(t) \rangle \sim At^{-(1+\delta)/(2-p)} |\ln(t/\tau)|^\alpha$, with
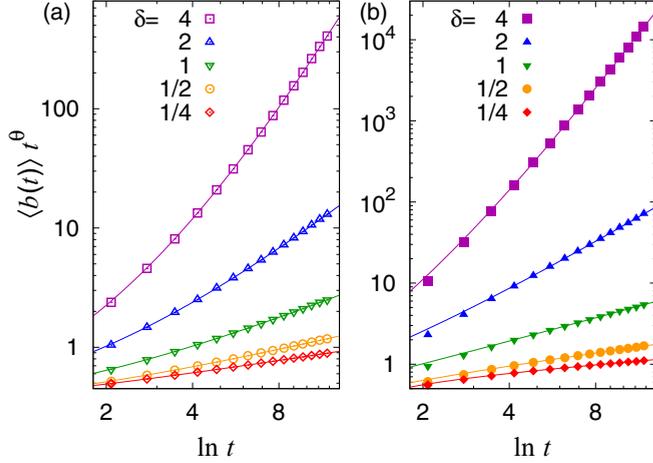
FIG. 10. Log-log plot of $\langle b(t) \rangle t^\theta$ versus $\ln t$ in $d = 2$ for (a) $p = 0$ and (b) $p = 1$, for various δ. The slope asymptotically approaches the value α. The solid lines are three-parameter fits, as described in the text.

fit parameters A, τ, and α. We chose $t_{\min} = 64$ for $p = 0$ and $t_{\min} = 256$ for $p = 1$, based on analysis of residuals. We find statistical uncertainties for the values of α of the order of 1%. The data and fits for $p = 0$ and 1 and a range of diffusion constant ratios δ are shown in Fig. 10. In Table III, the fitted values are listed in comparison to the RG calculated values from Rajesh and Zaboronski [8]. The agreement is striking.

Next we consider a finite local reaction rate λ' (for the trapping reaction) which, according to Eq. (23), should affect the value of α. We vary λ' by setting p', the probability of a B particle reacting upon landing at a site occupied by an A particle, to be less than unity. We find indeed that α is dependent on p', as shown in Table IV. Here α_0 corresponds to $p = 0$ and α_1 to $p = 1$.

For the special case of $\lambda \to \infty$ and $\delta = 1$, Eq. (23) becomes

$$\alpha = \frac{4 - 3p}{(2 - p)^2} + \frac{16\pi}{(2 - p)\lambda'}. \qquad (28)$$

The local reaction rate λ' is a coupling constant in the field theory (see Refs. [8,9]) and is influenced by the lattice constant, lattice type, hopping rules, etc., and cannot be simply determined from the model parameters. Nevertheless, Eq. (28)

TABLE III. Measured values of α in the limit of infinite local reaction rates for various diffusion constant ratios $\delta = D_B/D_A$ and trap reaction parameter p, defined in Eq. (1). The RG predictions are from Ref. [8].

	$p = 0$		$p = 1$	
δ	α_{measured}	α_{RG}	α_{measured}	α_{RG}
1/4	0.386(5)	0.3894	0.283(11)	0.2701
1/2	0.585(7)	0.5780	0.49(2)	0.4935
1	0.998(12)	1	0.97(3)	1
2	1.98(2)	1.974	2.13(4)	2.1808
4	4.35(2)	4.259	4.89(9)	4.9551

TABLE IV. Measured values of α for finite local reaction rate λ_B for $\delta = 1$ and various values of p'.

$1 - p'$	α_0	α_1	$(\alpha_1 - 1)/(\alpha_0 - 1)$
0	0.998(12)	0.97(3)	
1/8	1.49(2)	1.97(3)	2.00(4)
1/4	2.11(2)	3.22(3)	2.01(3)
1/2	4.27(3)	7.56(4)	2.01(2)

predicts that when all model parameters are unchanged except for the value of p, the ratio $(\alpha_1 - 1)/(\alpha_0 - 1) = 2$. This is confirmed by our data, as shown in Table IV.

The cross-correlation function $C_{AB}(r, t)$ is shown in Fig. 11 to exhibit the expected scaling form Eq. (26). As in the one-dimensional case, we find $C_{AB}(r, t)$ to be a nonmonotonic function of r when $p = 1$.

Finally, we turn to the anomalous dimension $\chi_{BB} \sim |\ln t|^\beta$. As shown in Fig. 12, we are not able to obtain clear scaling before the onset of finite-size effects. The data for $p = 0$ are consistent with the RG value $\beta = -5/12$ from Eq. (24), as shown in Fig. 12(a). However, the RG prediction for $p = 1$ is $\beta = 4/3$, i.e., χ_{BB} should be increasing with time, which is clearly inconsistent with the data. This discrepancy requires resolution.

While we have not reached the scaling regime for the B-particle correlations, we can nonetheless test for scaling collapse by rescaling $C_{BB}(r, t)$ by its value at $r = 0$, which is shown in Fig. 13. The scaling is noticeably better for $p = 0$ than for $p = 1$.

VII. SUMMARY

We have developed a hybrid simulation method for the coupled two-species reactions $A + B \to A$ and $A + A \to (0, A)$
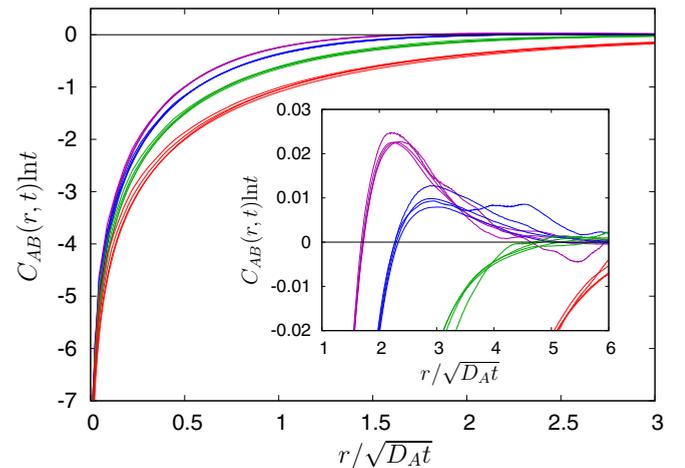

FIG. 11. Scaling plot of $C_{AB}(r, t) \times \ln t$ versus $r/\sqrt{D_A t}$ in $d = 2$ for four different parameter values: from top to bottom $(p, \delta) = (1, 1/4)$, $(1, 1)$, $(0, 1)$, and $(0,4)$. For each parameter value, the times $t = 2048, 8192, 32768$, and 131072 are shown to collapse to a single curve. The inset is the same plot with different ranges, to highlight the nonmonotonicity and positive correlation region for $p = 1$.
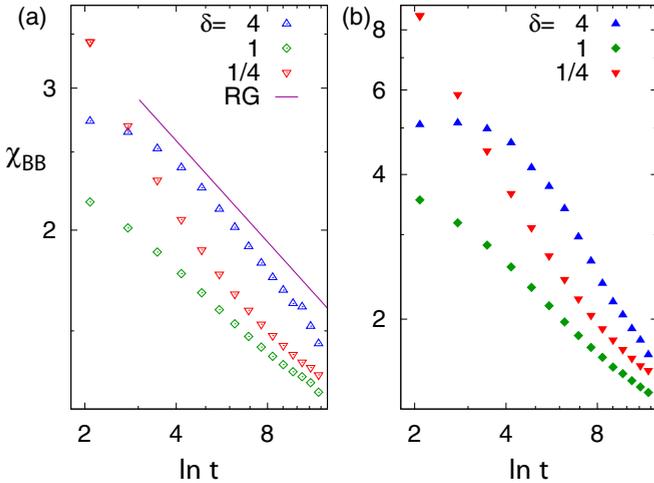
FIG. 12. Log-log plot of χ_{BB} versus $\ln t$ in $d = 2$ for (a) $p = 0$ and (b) $p = 1$, for various δ. The RG prediction from [9] is shown for $p = 0$. For $p = 1$ the predicted slope is positive, which is not consistent with the data.
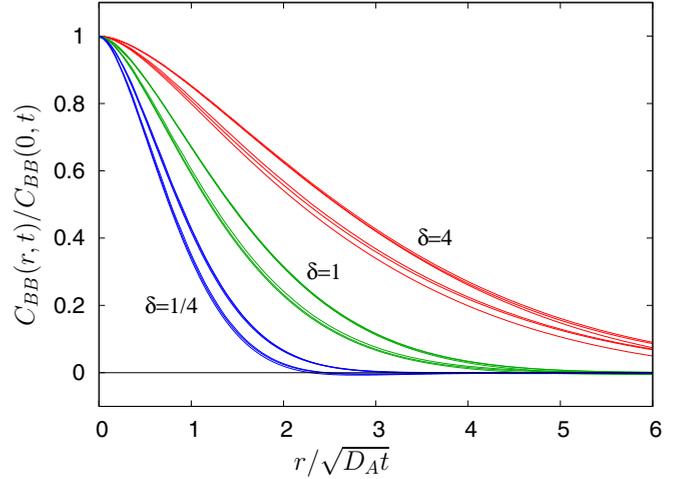

FIG. 13. Plot of $C_{BB}(r, t)$ versus $r/\sqrt{D_A t}$ in $d = 2$ with the vertical axis scaled to be unity at $r = 0$. The six curves are from top to bottom $(p, \delta) = (0, 4), (1, 4), (0, 1), (1, 1), (0, 1/4), (1, 1/4)$. For each parameter set, the times $t = 2048$, 8192, and $32\,768$ are plotted.

that involves a Monte Carlo simulation of the traps combined with the full probability distribution for the particles. This method provides significant improvement for statistics and avoids the problem of vanishing B particle numbers, and allows us to obtain what we believe are the first numerical measurements for this system with mobile B particles (Monte Carlo simulations with stationary B particles in $d = 2$ were conducted in Ref. [8]).

With this technique, we explored the behavior of this reaction-diffusion system for a variety of diffusion constant ratios and trap reaction types. In $d = 1$, we were able to obtain for all parameter values convincing power-law decay of the B-particle density and to measure the decay exponent to 0.1% accuracy, as shown in Table I. Our results are consistent with all known exact values. Our data were compared with theoretical results from the RG $\epsilon = 2 - d$ expansion and from Smoluchowski theory.

Also, in $d = 1$, we further tested the recently calculated anomalous dimension in the B-particle correlation function or, equivalently, in the local fluctuations of the B particles: $\chi_{BB} = C_{BB}(0, t) \sim t^{\phi}$. For the case of coalescing traps, we were able to obtain multiple decades of power-law scaling and measure the exponent ϕ to 0.5% accuracy (see Table II). Our measured values do not match the truncated RG calculation, but are consistent with one exact value.

We have also tested for universality by varying the trapping reaction probability p', defined in Eq. (9). We confirmed that the exponents θ and ϕ and the correlation functions are not dependent on this parameter, consistent with them being universal functions of δ and p. In contrast, the amplitude of the density decay $\langle b \rangle \sim A t^{-\theta}$ is dependent on p' and is nonuniversal.

It is noteworthy that the power-law behavior in the correlation function $C_{BB}(x, t)$ and fluctuations χ_{BB} encountered finite-size effects much earlier than the density $\langle b \rangle$. From Fig. 6, we see finite-size effects entering around $t = 3 \times 10^4$ for the equal diffusion constant case, at which time the diffusion length is $\sqrt{Dt} \sim 100$ in a system of size 3×10^7. The origin of this extreme sensitivity merits further investigation, both analytically and numerically.

In $d = 2$, the RG predicts logarithmic corrections to both the B-particle density and to χ_{BB}. We measured these exponents and found excellent agreement to density exponents θ and α calculated by Rajesh and Zaboronski [8], as shown in Table III. We observed scaling of the expected from $\chi_{BB} \sim |\ln t|^{\beta}$ consistent with the predicted value of β for the case $p = 0$, but our data are inconsistent with the RG prediction for the case $p = 1$. This discrepancy merits further study.

Finally, it will be interesting to see if this numerical technique has broader applications. In multispecies reaction schemes, whenever a particular species X is essentially a dynamic tracer that does not affect the behavior of the other species, as with the B particles in this study, it should be possible to obtain the full probability distribution of X by the method developed here. An open question that merits further investigation is whether this technique can be used for particles that are not initially random; i.e., whether other initial distributions will converge to the local Poissonian distribution.

[1] S. A. Rice, *Diffusion-Limited Reactions* (Elsevier, Amsterdam, 1985).

[2] J. Krug and H. Spohn, *Solids Far From Equilibrium*, edited by C. Godrèche (Cambridge University Press, Cambridge, 1991).

[3] J. L. Spouge, Phys. Rev. Lett. **60**, 871 (1988).

[4] A. J. Bray, Adv. Phys. **43**, 357 (1994).

[5] U. C. Täuber, J. Phys. A **45**, 405002 (2012).

[6] M. Howard, J. Phys. A **29**, 3437 (1996).

[7] S. Krishnamurthy, R. Rajesh, and O. Zaboronski, Phys. Rev. E **68**, 046103 (2003).

[8] R. Rajesh and O. Zaboronski, Phys. Rev. E **70**, 036111 (2004).

[9] B. Vollmayr-Lee, J. Hanson, R. S. McIsaac, and J. D. Hellerick, J. Phys. A: Math. Theor. **51**, 034002 (2018); **53**, 179501 (2020).

[10] M. Bramson and J. L. Lebowitz, Phys. Rev. Lett. **61**, 2397 (1988).

[11] A. J. Bray and R. A. Blythe, Phys. Rev. Lett. **89**, 150601 (2002).

[12] R. A. Blythe and A. J. Bray, Phys. Rev. E **67**, 041101 (2003).

[13] A. J. Bray, S. N. Majumdar, and G. Schehr, Adv. Phys. **62**, 225 (2013).

[14] D. C. Torney and H. M. McConnell, J. Phys. Chem. **87**, 1941 (1983).

[15] A. A. Lushnikov, Phys. Lett. A **120**, 135 (1987).

[16] V. Privman, *Nonequilibrium Statistical Mechanics in One Dimension* (Cambridge University Press, Cambridge, 1997).

[17] L. Peliti, J. Phys. A **19**, L365 (1986).

[18] B. P. Lee, J. Phys. A **27**, 2633 (1994).

[19] U. C. Täuber, M. Howard, and B. P. Vollmayr-Lee, J. Phys. A **38**, R79 (2005).

[20] P. L. Krapivsky, Phys. Rev. E **49**, 3233 (1994).

[21] B. Helenbrook and D. ben-Avraham, Phys. Rev. E **97**, 052105 (2018).

[22] V. Mehra and P. Grassberger, Phys. Rev. E **65**, 050101(R) (2002).

[23] M. E. Fisher and M. P. Gelfand, J. Stat. Phys. **53**, 175 (1988).

[24] M. Abramowitz and I. A. Stegun, *Handbook of Mathematical Functions* (Dover, New York, 1972).

[25] T. O. Masser and D. ben-Avraham, Phys. Rev. E **64**, 062101 (2001).

[26] B. P. Vollmayr-Lee and M. M. Gildner, Phys. Rev. E **73**, 041103 (2006).